Electronic Supplementary Information

Surface Plasmon-Induced Hot Carrier Effect on Catalytic Activity of CO oxidation on Cu_2O/Hexoctahedral Au Inverse Catalyst

Si Woo Lee,[a,b] Jong Wook Hong,[c,d] Hyunhwa Lee,[a,b] Dae Han Wi,[c] Sun Mi Kim,[a] Sang Woo Han,[c] and Jeong Young Park *[a,b]*

[a] Center for Nanomaterials and Chemical Reactions, Institute for Basic Science, Daejeon 34141, Republic of Korea

[b] Graduate School of EEWS, KAIST, Daejeon 34141, Republic of Korea

[c] Center for Nanotectonics, Department of Chemistry and KI for the NanoCentury, KAIST, Daejeon 34141, Republic of Korea

[d] Department of Chemistry, University of Ulsan, Ulsan 44610, Republic of Korea

*To whom correspondence should be addressed. E-mail: jeongypark@kaist.ac.kr, sangwoohan@kaist.ac.kr

KEYWORDS: Inverse catalyst, CO oxidation, cuprous oxide, HOH, hot electron injection, LSPR excitation

1. Arrhenius plots for CO oxidation of the Cu_2O/Au vertex site, HOH Au@Cu_2O, Cu_2O NPs, and HOH Au NCs catalysts.

Figure S1 shows the Arrhenius plots of the Cu_2O/Au vertex site, HOH Au@Cu_2O, Cu_2O, and HOH Au catalysts. The activation energies can be calculated from the slope of these Arrhenius plots, and the values for the Cu_2O/Au vertex site, HOH Au@Cu_2O, and Cu_2O nanoparticles were 15.8, 16.4, and 13.1 kcal/mol, respectively. Furthermore, the activation energy for Cu_2O was much lower than for the HOH Au NCs, which indicates that the HOH Au NCs were catalytically inactive for CO oxidation.

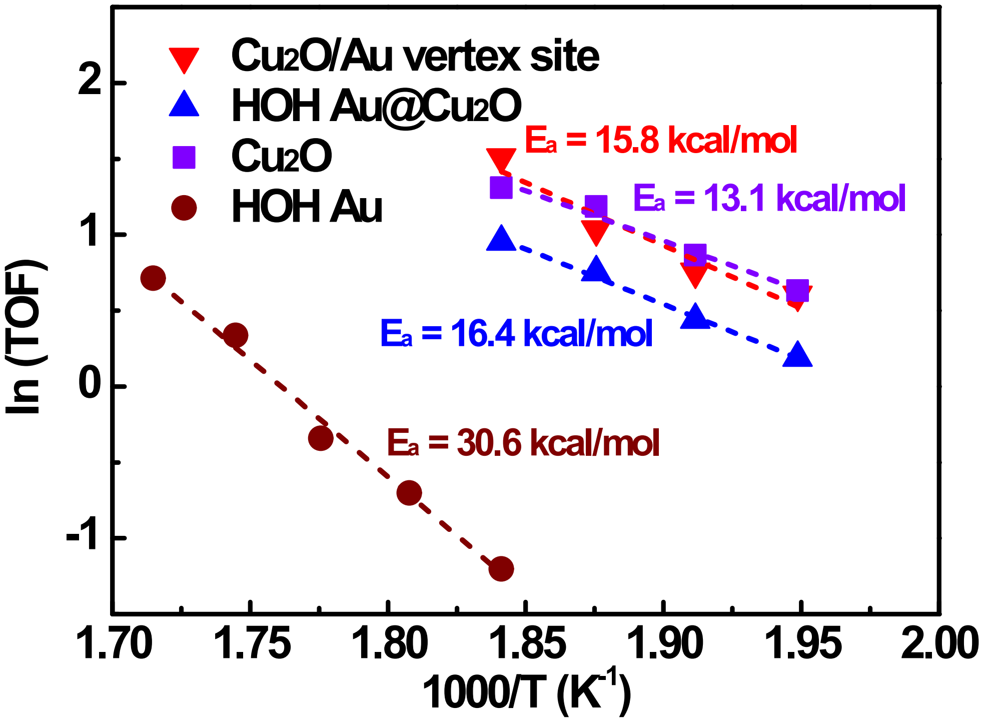

Figure S1. Arrhenius plots of the Cu_2O/Au vertex site, HOH Au@Cu_2O, Cu_2O, and HOH Au catalysts.

2. Structures of the Cu_2O at the Vertex Sites of the Hexoctahedral (HOH) Au Nanocrystals (Cu_2O/Au vertex site) and HOH Au–Cu_2O Core–Shell Structure (HOH Au@Cu_2O).

The morphologies of the Cu_2O/Au vertex site and HOH Au@Cu_2O were characterized using scanning electron microscopy (SEM, Magellan 400). The SEM images before and after one cycle of CO oxidation show that there was some change, but not a significant change, in the morphology of the Cu_2O/Au inverse catalyst.

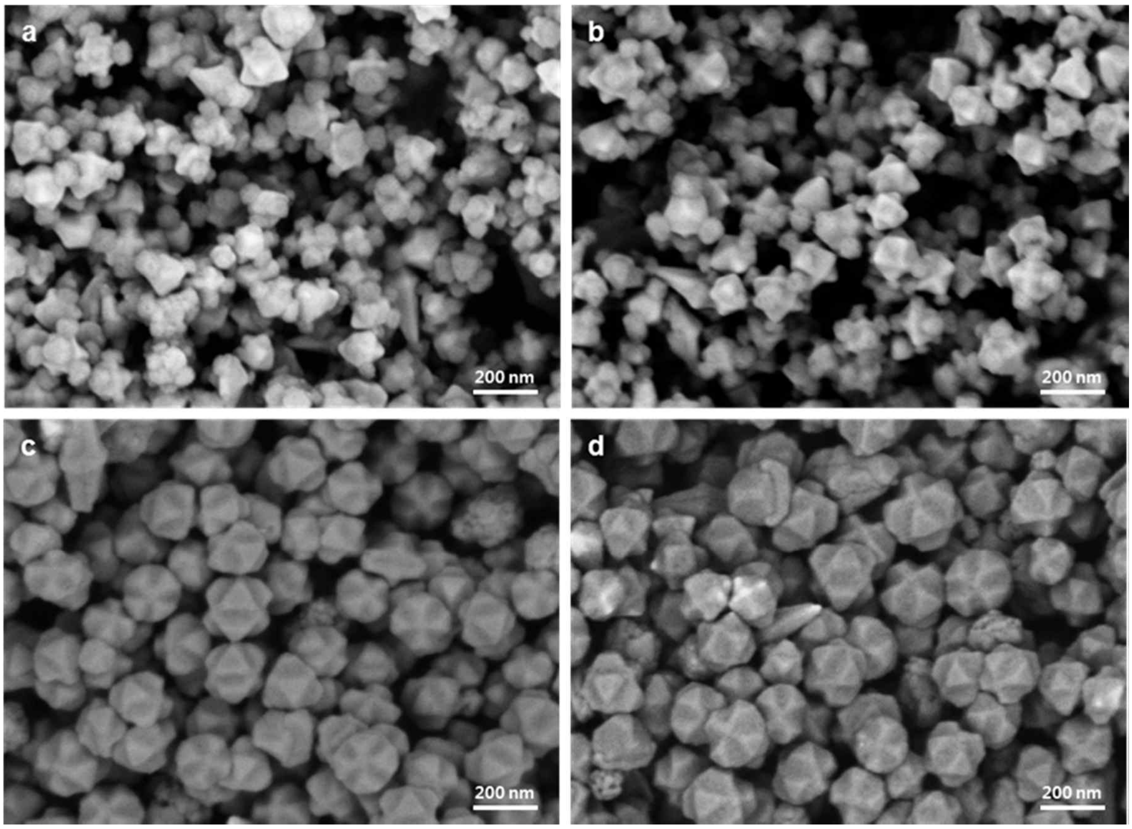

Figure S2. SEM images of the Cu_2O/Au vertex site (a) before and (b) after one cycle of CO oxidation and HOH Au@Cu_2O (c) before and (d) after one cycle of CO oxidation.

3. X-ray Photoelectron Spectroscopy (XPS) Spectra of the Cu_2O/Au Vertex Site.

Figure S3 shows the chemical state of the Au (Au 4f) and Cu_2O (Cu 2p) taken using X-ray photoelectron spectroscopy (XPS, Thermo VG Scientific Sigma Probe system with an Al Kα X-ray source (1486.3 eV)) before and after CO oxidation. The chemical state of the Au did not change and there was little oxidation of Cu^+ to Cu^{2+}, which is the less-reactive oxidation state of Cu-based catalysts; the dominant state was still Cu^+.

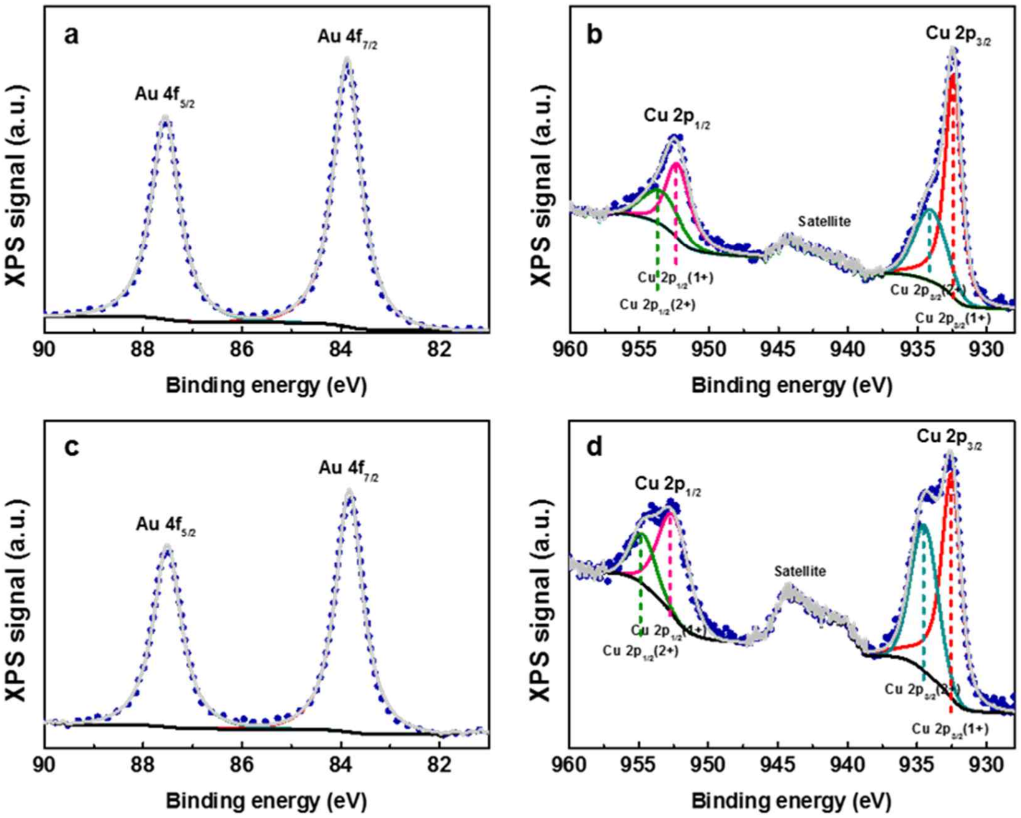

Figure S3. XPS spectra of Au 4f and Cu 2p on the Cu_2O/Au vertex site (a,b) before and (c,d) after CO oxidation, respectively.

4. Measurement of Catalytic Activity of CO Oxidation on Cu_2O/Au Vertex Site with and without Light at 523 K to Check the Reversible Hot Carrier Effect.

CO oxidation was carried out continuously on the Cu_2O/Au vertex site with and without light at 523 K. Figure S4 represents the continuous turnover frequency (TOF) for CO oxidation on the Cu_2O/Au vertex site with and without light at 523 K to check whether the effect of hot electron injection was reversible. The TOF value was similar to previous experimental results (Figure 3b), and the effect of hot carrier injection was reversible by observation of the enhancement and return of the catalytic activity as the halogen lamp was turned on and off, respectively.

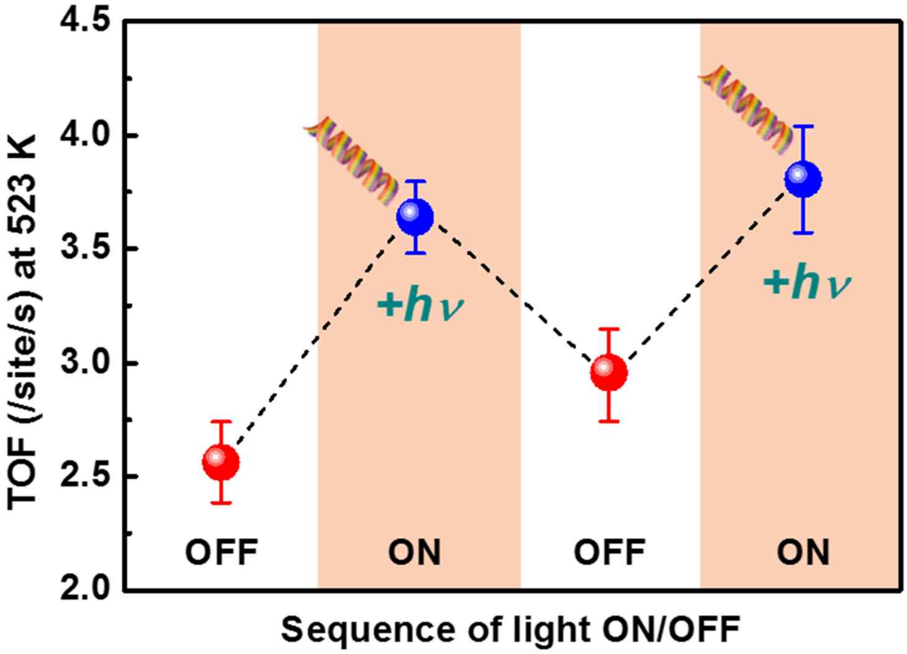

Figure S4. TOF for CO oxidation with a sequence of light ON/OFF on the Cu_2O/Au vertex site at 523 K. The TOF value was calculated from the slope of the turnover number with reaction time.

5. Finite-Difference Time Domain (FDTD) Simulations on the HOH Au, Cu_2O/Au Vertex Site, and HOH Au@Cu_2O.

Figure S5 shows the electric field distribution that indicates the enhancement of light absorption by LSPR excitation around the HOH Au, Cu_2O/Au vertex site, and HOH Au@Cu_2O with incident light of 750, 800, and 850 nm using two-dimensional FDTD simulation analysis.

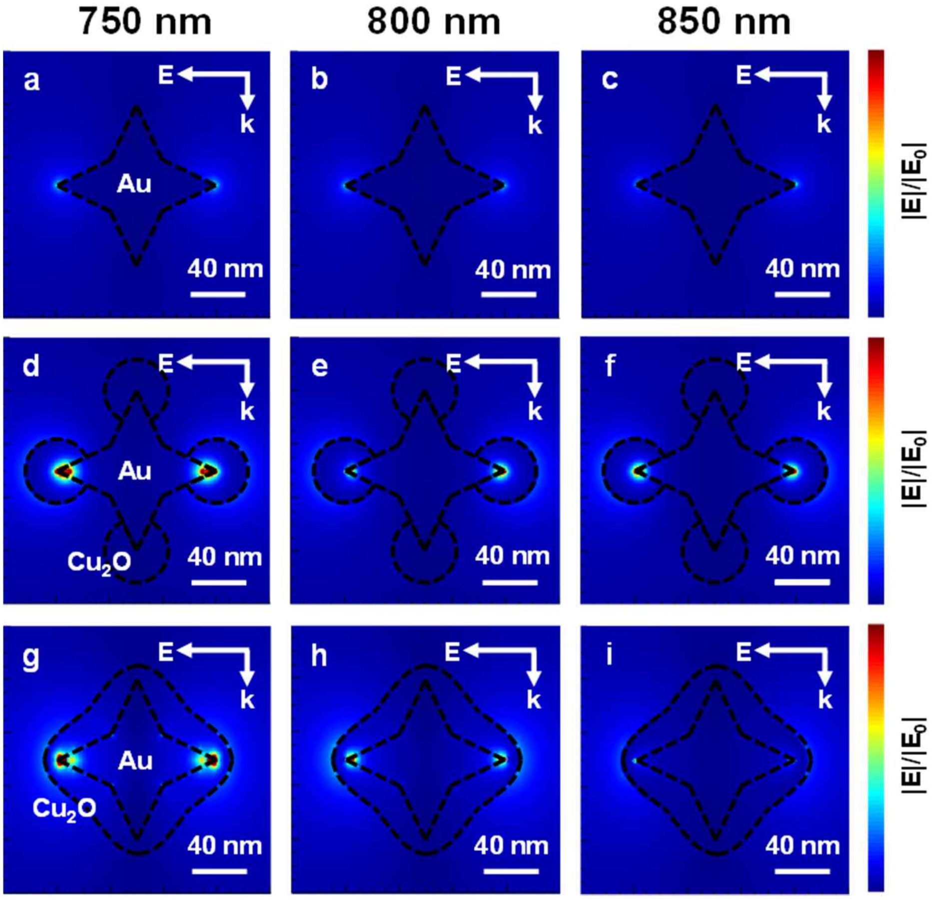

Figure S5. FDTD simulation of electric field distribution by LSPR excitation on (a–c) the HOH Au, (d–f) Cu_2O/Au vertex site, and (g–i) HOH Au@Cu_2O with incident light of 750, 800, and 850 nm.